

[Click to View Poster](#)

## **EA Impact of Shear Velocity Estimation on Wellbore Stability\***

**Charles Otoghile<sup>1</sup> and Chima Cyril Udeze<sup>1</sup>**

Search and Discovery Article #42351 (2019)\*\*

Posted February 4, 2019

\*Adapted from extended abstract prepared in conjunction with poster presentation given at 2018 International Conference and Exhibition, Cape Town, South Africa, November 4-7, 2018

\*\*Datapages © 2019 Serial rights given by author. For all other rights contact author directly. DOI:10.1306/42351Otoghile2019

<sup>1</sup>Software Integrated Solutions, Schlumberger, Lagos, Lagos, Nigeria ([cotoghile@slb.com](mailto:cotoghile@slb.com))

### **Abstract**

The main purpose of this study is to determine a shear velocity prediction scheme for deep offshore Niger Delta accurate enough for use in wellbore stability. There are few wells in the area that contain measured shear velocity data and these wells are located close to each other. Six (6) wells are utilized. The available logs were analyzed using Greenberg and Castagna and Mudrock line equations.

The aim is to determine how reliable the Greenberg and Castagna equation is in estimating shear velocity and to determine the locally calibration coefficients of the equation to use for similar lithologies in the Niger Delta. The results from the Greenberg and Castagna equation was further compared to the Mudrock line equation. The difference in the results further establish the importance of having locally calibrated coefficients when using the Greenberg and Castagna equation to estimate shear velocity.

### **Introduction**

The Greenberg - Castagna method was used to predict the Vs in the study area using a control well with known sand and shale coefficients. New lithologies i.e. sand and shale (illite, kaolinite, muscovite mica, and chlorite) coefficient were derived using the data from the wells in the study area. This new calibration shows that the locally calibrated coefficient gave a better result in estimating shear velocity than the widely accepted Greenberg - Castagna coefficient. The local sand and shale trends are also closer than the controlled sand and shale trend. Note: The coefficients from Greenberg - Castagna equation were derived from a global data set including Gulf of Mexico samples.

The linear relationship between Vp and Vs used by Greenberg and Castagna is:

$$V_s = A_0 + A_1 V_p \text{ for sand (1)}$$

$$V_s = B_0 + B_1 V_p \text{ for shale (2)}$$

where  $A_0=-0.85588$ ,  $A_1=0.80416$ ,  $B_0=-0.86735$ , and  $B_1=0.76969$ .

Mudrock line equation is:

$$V_p = 1.16V_s + 1.36$$

Where  $V_p$  and  $V_s$  refers to P-wave velocity and S-wave velocity.

The wells in the study area are located in the range of 2,953 ft – 3,937 ft water depth and are referred to as Well #1, Well #2, Well #3, Well #4, Well #5, and Well #6. Crossplots of the  $V_p$ - $V_s$  from Well #4 shows a linear relationship with some data points of the linear trend relationship. However, some data points outside the linear trend are due to the presence of hydrocarbon as shown in [Figure 1](#).

### Method

Petrophysical analysis was carried out in the study area and a robust lithologic model was developed. This model captures the volume of key minerals (quartz, illite, kaolinite, muscovite mica, and chlorite) in the study area. The Greenberg - Castagna  $V_p$ - $V_s$  approach is lithology dependent.

A Gassmann fluid substitution of 100% brine saturation was performed on the key logs ( $V_p$ ,  $V_s$ , density). Fluid properties were computed as this is a key component for fluid substitution ([Figure 2](#), [Figure 2a](#), and [Figure 2b](#)). Elastic properties (Poisson's Ratio, Young's Modulus, Bulk Modulus, and  $V_p/V_s$ ) were also computed. The model was calibrated by adapting the constant/linear and quadratic factors of the Greenberg - Castagna equation for each of the minerals. Zones were defined for shales, hydrocarbon bearing sands, and wet sands. This was done to improve the calibration of the coefficient for each of the defined rock units/zones. These calibrated models were applied to other wells excluded from the calibration model to verify the accuracy of the prediction.

### Results

The results of the study show the importance of having a locally calibrated coefficient for the Greenberg – Castagna equation ([Figure 3](#)). The results show a good match between the measured  $V_s$  and the modeled  $V_s$  ([Figure 4](#), [Figure 5](#), and [Figure 6](#)).

### Discussion

From the analysis a good trend was observed between the measured  $V_s$  and the modeled  $V_s$  ([Figure 7](#)). This is an indication that the coefficient that was generated fit the shear velocity trend for computation of the Greenberg – Castagna equation locally i.e. Niger Delta. In addition, the Mudrock line equation was also used to compute shear velocity and this was compared to the result of the study. The result of the Mudrock line indicates an over estimation of the shear velocity as seen in [Figure 8](#).

## **Conclusions**

The locally calibrated coefficient shows a close match for Vs compared to the measured Vs. Even though these values are localized, they produce better Vs estimates in a test well. Shear slowness is a key component of the mechanical earth modeling because it is an important input when computing elastic parameters such as Young's Modulus and Poisson's Ratio. An over estimation or under estimation of shear slowness will have a huge impact on the final wellbore stability model.

## **Selected References**

- Henning, A., and G. Powers, 2000, Shear-Wave Velocity Estimation in the Deepwater Gulf of Mexico: 2000 SEG Annual Meeting, 6-11 August, Calgary, Alberta, SEG-2000-1723, 4 p.
- Castagna, J.P., M.L. Batzle, and R.L. Eastwood, 1985, Relationships Between Compressional-Wave and Shear-Wave Velocities in Clastic Silicate Rocks: *Geophysics*, v. 50/4, p. 571-581.
- Corredor, F., J.H. Shaw, and F. Bilotti, 2005, Structural Styles in the Deep-Water Fold and Thrust Belts of the Niger Delta: *American Association of Petroleum Geologists Bulletin*, v. 89/6, p. 753-780. doi:10.1306/02170504074
- Onuoha, K.M., 1999, Structural Features of Nigeria's Coastal Margin: An Assessment Based on Age Data from Wells: *Journal of African Earth Sciences*, v. 29/3, p. 485-499. doi:10.1016/S0899-5362(99)00111-6
- Tuttle, M.L.W., M.E. Brownfield, and R.R. Charpentier, 1999, Tertiary Niger Delta (Akata-Agbada) Petroleum System (No. 701901), Niger Delta Province, Nigeria, Cameroon, and Equatorial Guinea, Africa: U.S. Geological Survey, Open-File Report 99-50-H, 41 p.

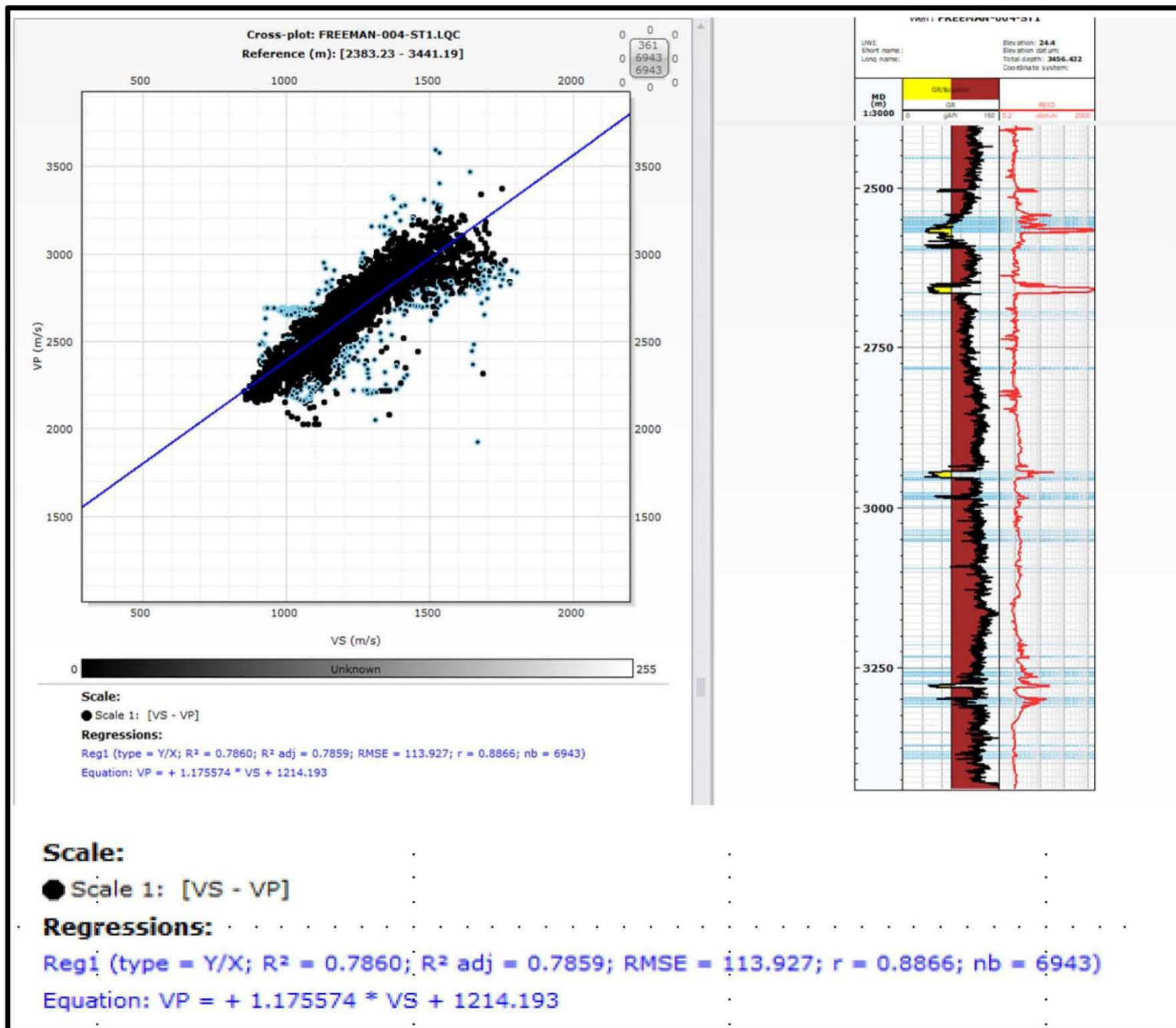


Figure 1. Showing crossplot of  $V_p - V_s$  relationship.



| Method settings                                   |              |              |              |                   |                 |                         |
|---|--------------|--------------|--------------|-------------------|-----------------|-------------------------|
| Gassmann fluid substitution from logs             |              |              |              |                   |                 |                         |
| save and display                                  |              |              |              |                   |                 |                         |
| Inputs  | Zonation     | Cut-Off      | Fluid Mixing | Mineralogy Mixing | Post-processing | Component specification |
|   | 1            | 2            | 3            | 4                 | 5               | 6                       |
| Use   | yes          | yes          | yes          | yes               | yes             | yes                     |
| Group   | 2- main      |              | 2- main      | 2- main           | 2- main         | 2- main                 |
| Well  | FREEMAN-001  | FREEMAN-002  | FREEMAN-003  | FREEMAN-003-ST1   | FREEMAN-005     | FREEMAN-004-ST1         |
| Dataset   | LQC          | LQC          | LQC          | LQC               | LQC             | LQC                     |
| Bulk Density                                      | DEN          | DENSITY      | DENSITY      | DENSITY           | DENSITY         | DENSITY                 |
| Total Porosity                                    | PHIT_ND      | PHIT_QE      | PHIT_ND      | PHIT_QE           | PHIT_QE         | PHIT_QE                 |
| Compressional Slowness                            | DT           | DTC          | DTC          | DTC               | DTC             | DTC                     |
| Shear Slowness                                    | DTS          | DTS          | DTS          | DTS               | DTS             | DTS                     |
| Initial Water Saturation                          | SW_QE        | SW_QE        | SW_QE        | SUWI_QE           | SUWI_QE         | SW_QE                   |
| Mineral Volume Fraction_Clay Volume Fraction      | VCL_GEO_QE   | VCL_GEO_QE   | VCL_GEO_QE   | VCL_GEO_QE        | VCL_GEO_QE      | VCL_GEO_QE              |
| Mineral Volume Fraction_Chlorite Volume Fraction  | Chlorite_QE  | Chlorite_QE  | Chlorite_QE  | Chlorite_QE       | Chlorite_QE     | Chlorite_QE             |
| Mineral Volume Fraction_Illite Volume Fraction    | Illite_QE    | Illite_QE    | Illite_QE    | Illite_QE         | Illite_QE       | Illite_QE               |
| Mineral Volume Fraction_Kaolinite Volume Fraction | Kaolinite_QE | Kaolinite_QE | Kaolinite_QE | Kaolinite_QE      | Kaolinite_QE    | Kaolinite_QE            |
| Mineral Volume Fraction_Muscovite Volume Fraction | Musc-Mica_QE | Musc-Mica_QE | Musc-Mica_QE | Musc-Mica_QE      | Musc-Mica_QE    | Musc-Mica_QE            |
| Mineral Volume Fraction_Quartz Volume Fraction    | Quartz_QE    | Quartz_QE    | Quartz_QE    | Quartz_QE         | Quartz_QE       | Quartz_QE               |

Figure 2. Showing Gassmann fluid substitution of 100% brine.

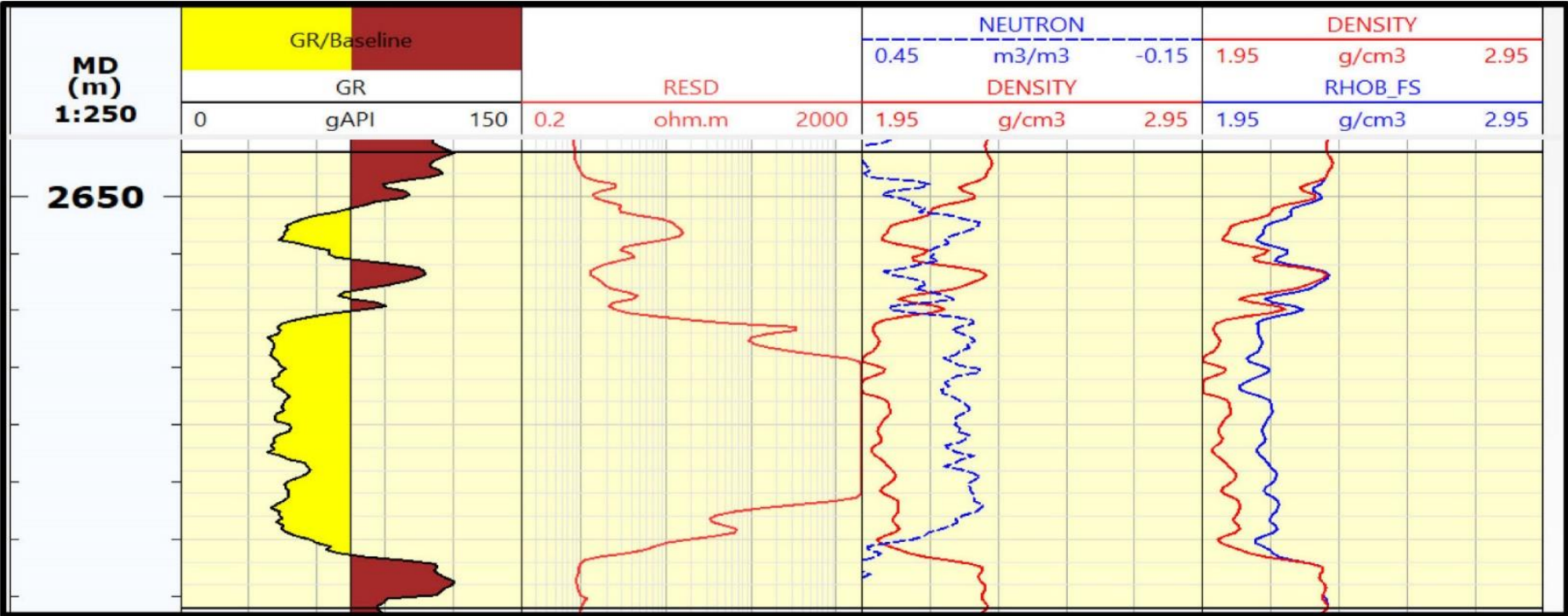


Figure 2a. Showing Gassmann fluid substitution of 100% brine.

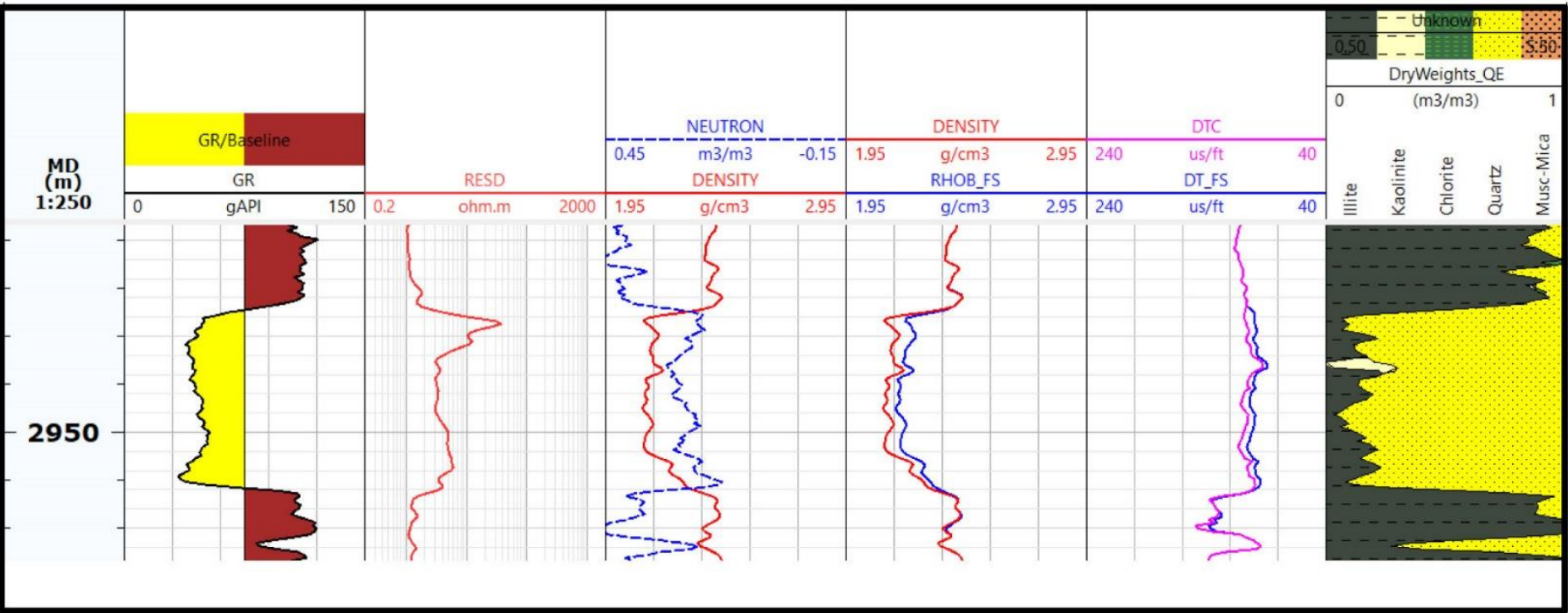


Figure 2b. Gassmann fluid substitution showing gas effect on the mineral.

|                                | Well #1              | Well #1         | Well #1     | Well #1     | Well #1          | Well #4          | Well #4          |
|--------------------------------|----------------------|-----------------|-------------|-------------|------------------|------------------|------------------|
| Dataset                        | LQC                  | LQC             | LQC         | LQC         | LQC              | LQC              | LQC              |
| Zone                           | Shale 1              | wet sand        | Oil Sand    | Shale 2     | Shale 1          | Oil Sand         | Shale 2          |
| Top                            | 3099.89              | 1583.489        | 3602.284    | 3651.448    | 2393.605         | 2501.575         | 2593.238         |
| Bottom                         | 3407.165             | 2067.446        | 3651.448    | 4120.042    | 2501.575         | 2506.886         | 2648.046         |
| Optimize                       | Quartz quadratic ... | Quartz quadr... | Quartz q... | Quartz q... | Quartz quadra... | Quartz quadra... | Quartz quadra... |
| Quartz quadratic coefficient   | 0.364117             | 0.250895        | -0.158975   | -0.139388   | 0.364117         | -0.158975        | -0.139388        |
| Quartz linear coefficient      | -1.00167             | -1.21936        | 1.70757     | 1.7686      | -1.00167         | 1.70757          | 1.7686           |
| Quartz constant                | 1.2812               | 2.11182         | -2.14303    | -2.48821    | 1.2812           | -2.14303         | -2.48821         |
| Shale quadratic coefficient    | -0.235079            | 1.49698         | -0.0596675  | -0.084599   | -0.235079        | -0.0596675       | -0.084599        |
| Shale linear coefficient       | 1.88333              | -5.19973        | 1.08327     | 1.16387     | 1.88333          | 1.08327          | 1.16387          |
| Shale constant                 | -2.122               | 5.11545         | -1.22976    | -1.27943    | -2.122           | -1.22976         | -1.27943         |
| Calcite quadratic coefficient  | -0.05508             | -0.05508        | -0.05508    | -0.05508    | -0.05508         | -0.05508         | -0.05508         |
| Calcite linear coefficient     | 1.01677              | 1.01677         | 1.01677     | 1.01677     | 1.01677          | 1.01677          | 1.01677          |
| Calcite constant               | -1.03049             | -1.03049        | -1.03049    | -1.03049    | -1.03049         | -1.03049         | -1.03049         |
| Dolomite quadratic coefficient | 0                    | 0               | 0           | 0           | 0                | 0                | 0                |
| Dolomite linear coefficient    | 0.58321              | 0.58321         | 0.58321     | 0.58321     | 0.58321          | 0.58321          | 0.58321          |
| Dolomite constant              | -0.07775             | -0.07775        | -0.07775    | -0.07775    | -0.07775         | -0.07775         | -0.07775         |

Figure 3. Calibration of the Greenberg – Castagna coefficient.



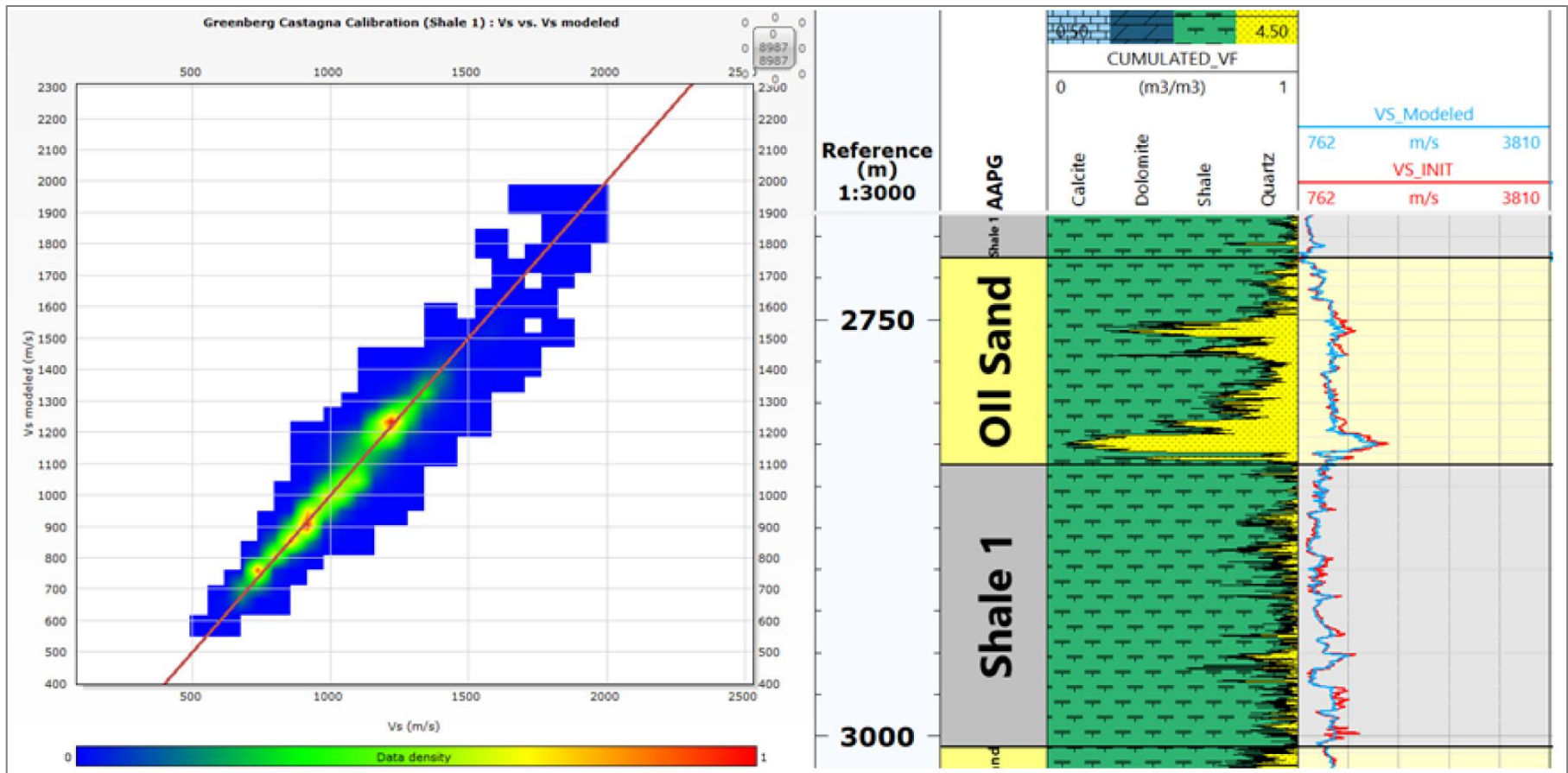


Figure 4. Crossplot of Vs modeled vs Vs measured for well #1.





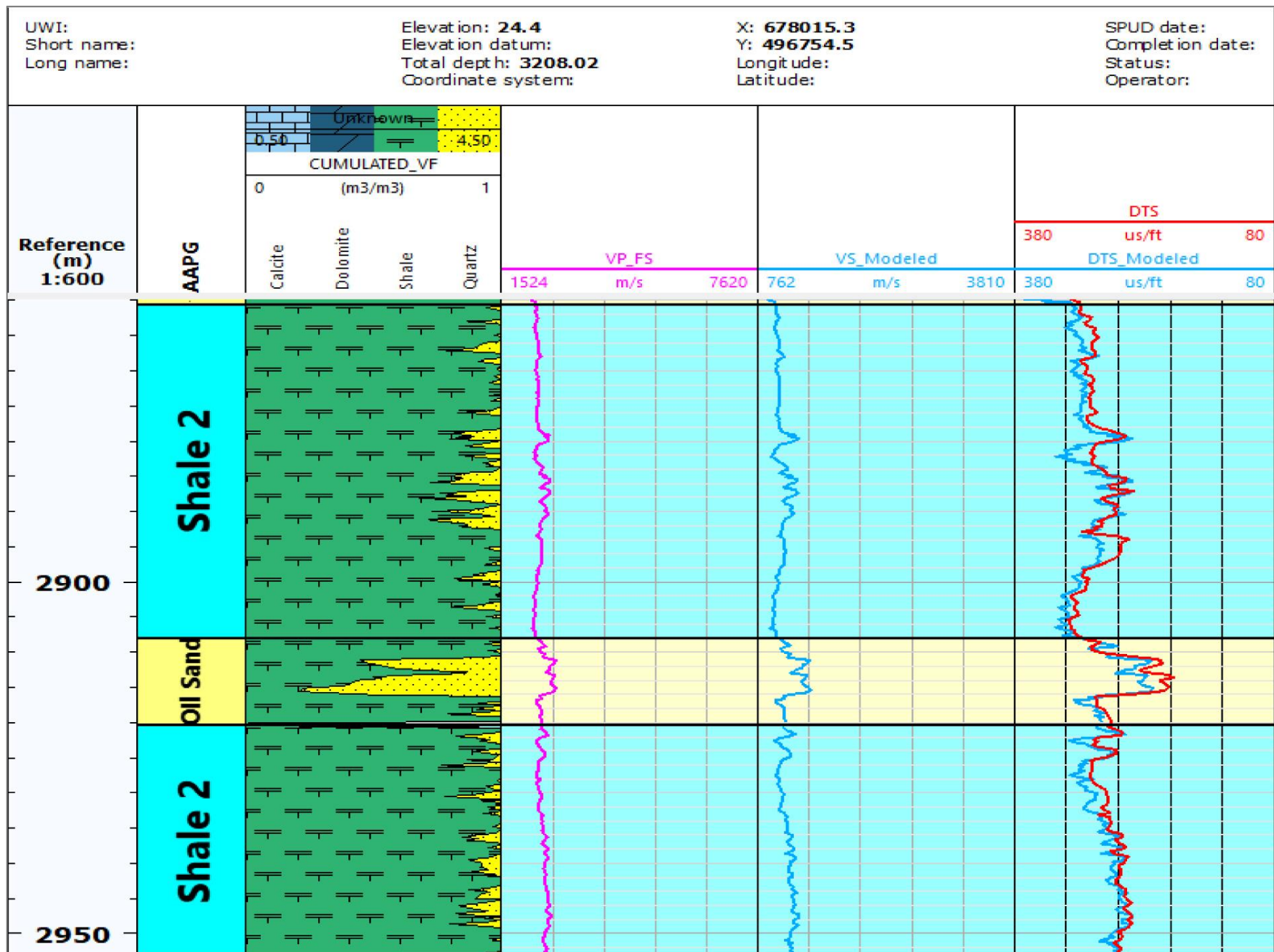


Figure 6. Showing application of the calibrated on Well #3. Note shows close match between the predicted DTS and measured DTS.

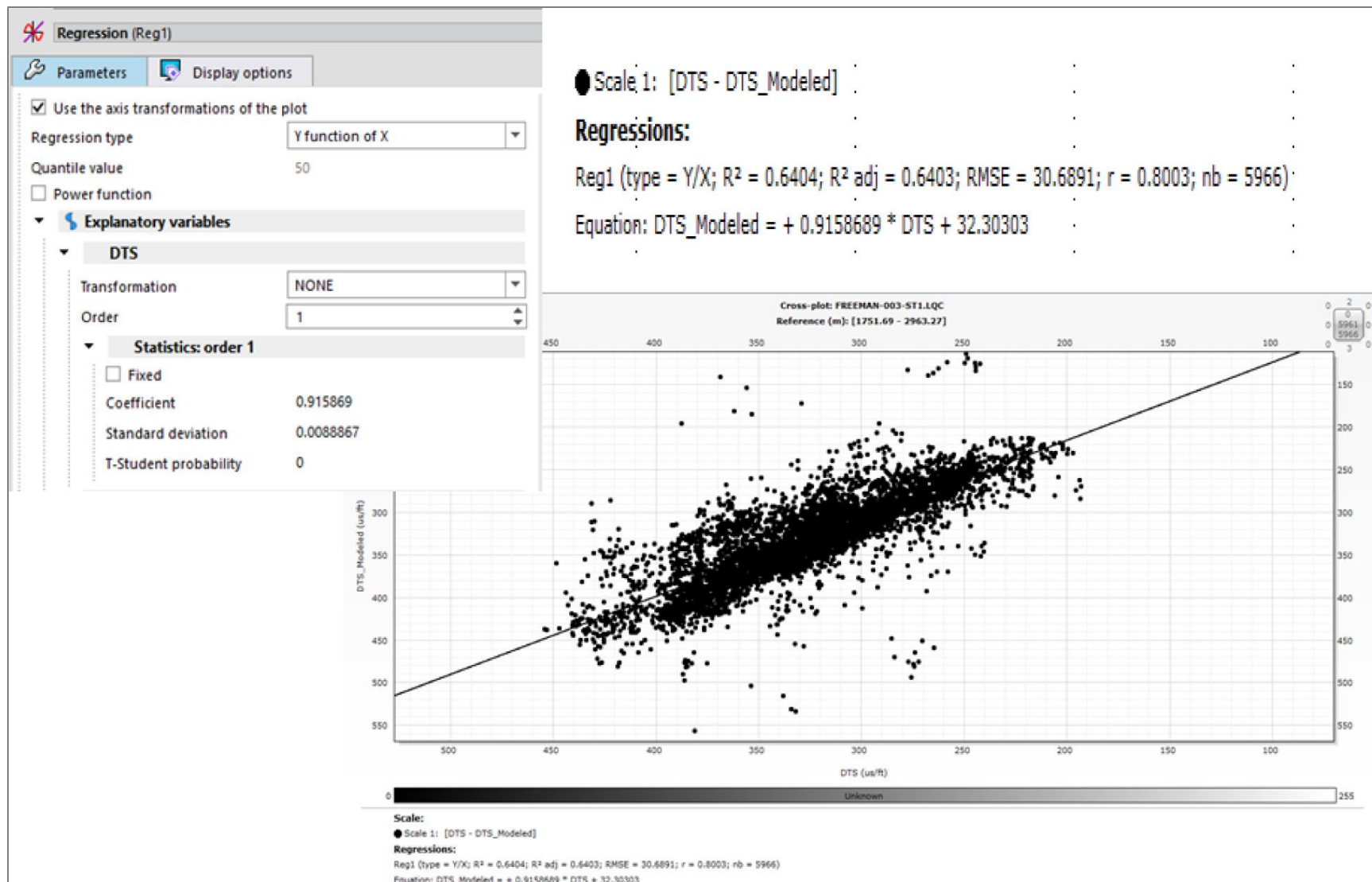


Figure 7. Showing the crossplot of the measured vs predicted.

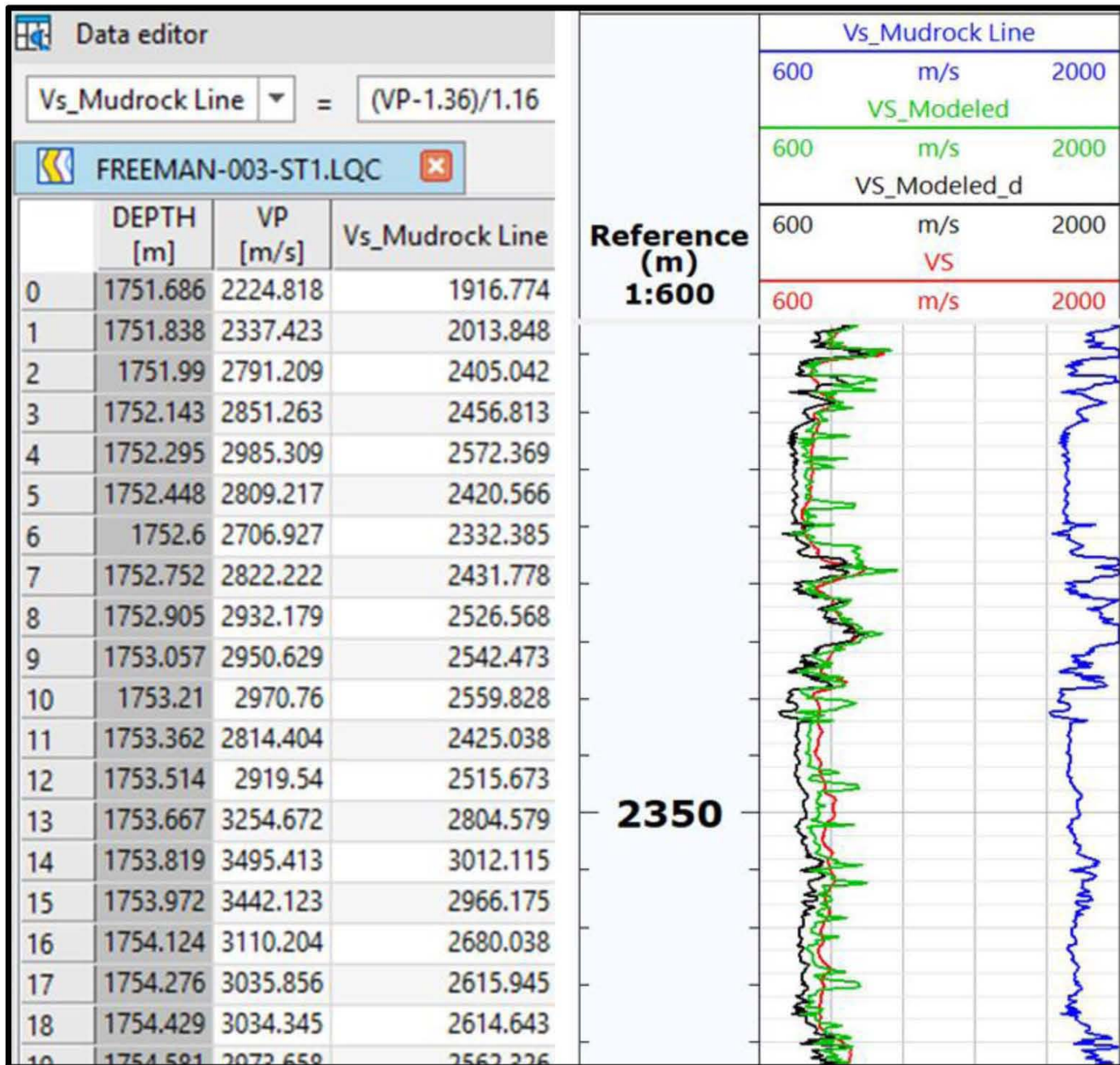


Figure 8. Mudrock line comparison with modeled Vs.